Unfolding mechanism of a hyperthermophilic protein O^6-methylguanine-DNA methyltransferase

Shingo Nishikori[a], Kentaro Shiraki[b], Shinsuke Fujiwara[c],
Tadayuki Imanaka[d], Masahiro Takagi[a],*

[a]School of Materials Science, Japan Advanced Institute of Science and Technology, 1-1 Asahidai, Tatsunokuchi, Ishikawa 923-1292, Japan
[b]Institute of Applied Physics, University of Tsukuba, 1-1-1 Tennodai, Tsukuba, Ibaraki 305-8573, Japan
[c]Department of Bioscience, School of Science and Technology, Kwansei-Gakuin University, 2-1 Gakuen Sanda, Hyogo 669-1337, Japan
[d]Department of Synthetic Chemistry and Biological Chemistry, Graduate School of Engineering, Kyoto University,
Katsura, Nishikyo-ku, Kyoto 615-8510, Japan

Abstract

Unfolding intermediates have been found only rarely in earlier studies, and how a protein unfolds is therefore poorly understood. In this paper, we show experimental evidence for multiple pathways and multiple intermediates during unfolding reaction of O^6-methylguanine-DNA methyltransferase from hyperthermophile *Thermococcus kodakaraensis* (*Tk*-MGMT). The unfolding profiles monitored by far-UV CD and tryptophan fluorescence were both biphasic, and unfolding monitored by fluorescence was faster than that monitored by CD. GdnHCl-induced titration curves indicate that the intermediates with significant α-helical structure accumulate during unfolding. Dependence of kinetic phases on initial GdnHCl concentrations and cysteine reactivity of *Tk*-MGMT were investigated, suggesting that the heterogeneity of native conformations and parallel unfolding pathways.
© 2005 Elsevier B.V. All rights reserved.

1. Introduction

Understanding how a protein folds to a unique three-dimensional structure is a major challenging issue in molecular structural biology. According to the traditional view, all unfolded protein molecules fold via essentially the same sequence to a unique native structure, while a 'new' view of protein folding has emerged from recent theoretical advances [1,2]. The 'new' view of folding replaces the folding pathways with that of energy landscapes, in which the folding intermediates and transition states are of many different forms and are not unique structures [3,4].

However, there has been little experimental evidence for multiple equivalent folding pathways to support this new view. Furthermore, how a protein unfolds is especially poorly understood. It is commonly believed that there are no detectable intermediates in the kinetic unfolding reactions of small proteins. The basic reason is that unfolding monitored by optical probes follows a single exponential curve, and the same unfolding curve is produced by the monitoring probes either of the secondary structure or of the tertiary structure [5]. However, this common perception has been becoming demonstrated to be erroneous using NMR [6]. Although several studies have reported that kinetic

 * Corresponding author. Tel.: +81 761 51 1650; fax: +81 761 51 1655.
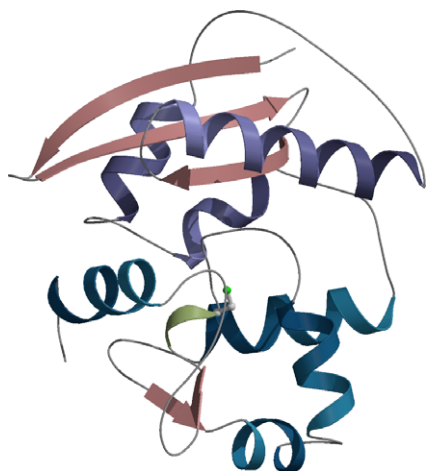 *E-mail address:* takagi@jaist.ac.jp (M. Takagi).

Fig. 1. Ribbon model of the crystal structure of *Tk*-MGMT. The active site of cysteine is illustrated by the ball-and-stick model.

intermediates actually accumulate in the unfolding pathway [7–9], there is still little information about the unfolding intermediate. Investigating the structural features of unfolding intermediates would not only enhance our understanding of the mechanism of protein folding, but would also provide clues to the interplay of molecular forces in many natural folding and disease-related misfolding processes. It is therefore important to understand the unfolding mechanism of proteins.

We have been studying a stability of a hyperthermophilic protein using O^6-methylguanine-DNA methyltransferase from hyperthermophilic archaeon *Thermococcus kodakaraensis* strain KOD1 (*Tk*-MGMT, EC 2.1.1.63) as a model protein. *Tk*-MGMT is a monomeric α/β protein, and consists of 174 amino acid residues with molecular weight of 19,500 (Fig. 1) [10,11]. *Tk*-MGMT becomes model systems to study the folding mechanism of proteins. First, *Tk*-MGMT is one of the most stable proteins. The melting temperature of *Tk*-MGMT was 108 °C, which was 55 °C higher than that of its mesophilic counterpart of AdaC. The maximum free energy change of *Tk*-MGMT was 42.9 kJ mol^{-1}, which was 2.6 times higher than that of AdaC [12]. Second, *Tk*-MGMT showed slow unfolding kinetics than AdaC and other mesophilic proteins [unpublished data]. Therefore, it is possible to detect the unstable intermediate during unfolding, and to analyze the unfolding mechanism in detail. In fact, we previously reported that unfolding kinetics of *Tk*-MGMT was not monophasic [13]. In this paper, we report the result of GdnHCl-induced kinetic and equilibrium unfolding studies of *Tk*-MGMT, aimed at a detailed characterization of the unfolding pathway. We reveal that there are multiple intermediate and multiple pathways in the unfolding reaction.

2. Materials and methods

2.1. Expression and purification of Tk-MGMT

Recombinant *Tk*-MGMT was expressed by IPTG induction in HMS174 (DE3) pLysS cells and purified to homogeneity as described previously [10]. The homogeneity of the purified protein was confirmed by SDS-PAGE. Protein concentrations were determined using a molar absorption coefficient of 18,000 M^{-1} cm^{-1} at 280 nm [14].

2.2. Equilibrium studies

Equilibrium refolding and unfolding as a function of GdnHCl concentration was monitored by far-UV CD and fluorescence. CD studies were conducted using a Jasco J-720 spectropolarimeter (Japan Spectroscopic Company, Tokyo, Japan). Spectra were collected with a bandwidth of 2 nm, a response time of 1 s, and a scan speed of 500 nm min^{-1}. Each spectrum was an average of at least 5 scans. Measurement was made with a protein concentration of 0.1 mg ml^{-1} with a 1-cm pathlength cuvette.

Fluorescence studies were conducted using a Jasco FP-6500 spectrofluorometer. To study the intrinsic fluorescence, the protein was excited at 280 nm, and emission was monitored from 300 nm to 450 nm with a slit width of 1 nm for excitation and 10 nm for emission. Spectra were collected with a response time of 1 s and a scan speed of 1000 nm min^{-1}. Each spectrum was an average of at least 5 scans. Measurement was made with a protein concentration of 0.1 mg ml^{-1} and a 1-cm pathlength cuvette.

Assuming a two-state transition, the equilibrium data were fitted by nonlinear least-square analysis using a two-state model. The observed signals (A_{obs}) at any concentration of GdnHCl are given by the following equation:

$$A_{obs} = \frac{A_N + A_U \exp\left\{-\left(\Delta G_{NU}^0 - m_{NU}[\text{GdnHCl}]\right)/RT\right\}}{1 + \exp\left\{-\left(\Delta G_{NU}^0 - m_{NU}[\text{GdnHCl}]\right)/RT\right\}}$$

(1)

where R and T are the gas constant and the absolute temperature, respectively, A_N and A_U are signals in the N and the U states, respectively, which are assumed to be linear dependence of [GdnHCl], and ΔG_{NU}^0 is free energy changes from N to U at 0 M GdnHCl.

Assuming a three-state transition, the observed signals of the protein (A_{obs}) at any concentration of the denaturant are given by the following equation:

$$A_{obs} = \frac{A_N + A_I \exp\left\{-\left(\Delta G_{NI}^0 - m_{NI}[\text{GdnHCl}]\right)/RT\right\} + A_U \exp\left\{-\left(\Delta G_{NU}^0 - m_{NU}[\text{GdnHCl}]\right)/RT\right\}}{1 + \exp\left\{-\left(\Delta G_{NI}^0 - m_{NI}[\text{GdnHCl}]\right)/RT\right\} + \exp\left\{-\left(\Delta G_{NU}^0 - m_{NU}[\text{GdnHCl}]\right)/RT\right\}}$$

(2)

where A_N, A_I, and A_U are the signals of the N, I, and U states, m_{NI} and m_{NU} represent the cooperative indexes of the respective transitions, and ΔG_{NI}^0 and ΔG_{NU}^0 are free energy changes from N to I and free energy changes from N to U at 0 M GdnHCl, respectively.

2.3. Kinetic studies

All measurements were made by manual mixing with a dead time of 5 s. A cuvette with a 1-cm pathlength was used for the CD and fluorescence measurements. The time courses of the unfolding of *Tk*-MGMT was followed by monitoring CD signals at 222 nm and fluorescence at 355 nm excited at 280 nm as a function of time. The final protein concentrations were 0.1 mg ml^{-1}. All the solutions contained 20 mM Tris–HCl (pH 8.0) with the desired concentrations of GdnHCl. The kinetic data for unfolding were fitted using a non-linear least-squares method with following equation:

$$A(t) = A_0 + A_1 \sum \alpha_i \exp(-k_1 t) \qquad (3)$$

where $A(t)$, A_0, and A_1 are the observed amplitude at time t, the amplitude at dead-end time, and total amplitude, respectively; k_i is the rate constant at the ith kinetic phase; and α_i is the fractional amplitude at the ith kinetic phase.

The kinetic data are interpreted by Eyring formalism [15], defining the activation free-energy change ($\Delta G^\ddagger$) as an explicit thermodynamic state. Rate constant k was determined by that activated state:

$$k = (\kappa k_B T / h) \exp(-\Delta G^\ddagger / RT) \qquad (4)$$

where κ is the transmission coefficient (usually set to unity), k_B is the Boltzmann constant (1.381×10^{-23} J K^{-1}) and h, the Planck constant (6.626×10^{-34} J s).

The resulting $\Delta G^\ddagger$ consists of the activation enthalpy change ($\Delta H^\ddagger$), the activation entropy change ($\Delta S^\ddagger$), and the heat capacity change upon activation ($\Delta C_p^\ddagger$), referring to a standard temperature at 298 K:

$$\Delta G^\ddagger(T) = \Delta H^\ddagger - T\Delta S^\ddagger$$
$$+ \Delta C_p^\ddagger((T - 298) - T\ln(T/298)). \qquad (5)$$

2.4. Reactions of cysteine residues in Tk-MGMT with DTNB

Fully folded protein was reacted with dithionitrobenzoic acid (DTNB) at pH 8.0. The protein was mixed with the buffer solutions (20 mM Na-phosphate, 1 mM EDTA, pH 8.0) containing 100 μM of DTNB by manual mixing (final protein concentration is 6.5 μM), and the increase in TNB$^-$ was monitored by absorbance at 412 nm using a Jasco V-550 spectrophotometer at 20 °C.

3. Results

3.1. Equilibrium transitions

Unfolding titration curves of *Tk*-MGMT were obtained at 20 °C by measuring the CD signals at 222 nm and the red shift of the emission wavelength of fluorescence excited at 280 nm. Fig. 2A shows the unfolding transition curves after incubation at 20 °C for 2 days. Complete unfolding equilibrium was not achieved even at 7.2 M GdnHCl, and CD and fluorescence signals were not superimposed. These results indicate that *Tk*-MGMT has an extremely slow rate of unfolding and that loss in the secondary and tertiary structures did not occur simultaneously. Fig. 2B shows the unfolding transition curves after incubation at 20 °C for 3 weeks. The unfolding data measured by fluorescence were fitted well to the two-state mechanism (Eq. (1)), while the unfolding data measured by CD at 222 nm were not fitted to the two-state mechanism, but were fitted well to the three-state mechanism (Eq. (2)), suggesting that unfolding proceeds
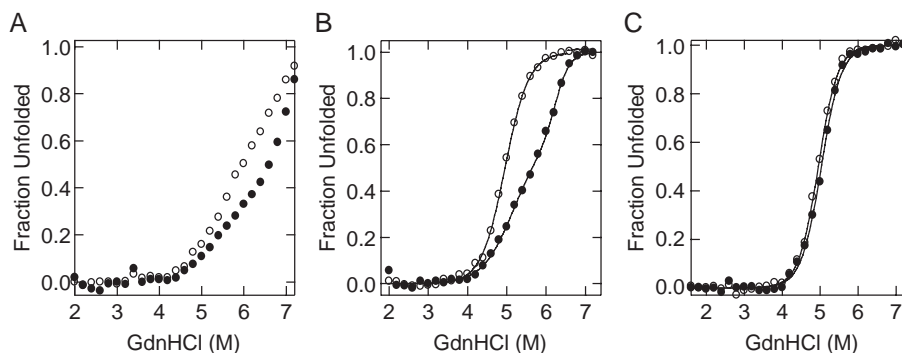

Fig. 2. GdnHCl-induced unfolding titration curves obtained by monitoring CD signals at 222 nm (closed circles) and the red shift of the maximum emission wavelength excited at 280 nm (open circles) at 20 °C. (A) Samples were equilibrated for 2 days at 20 °C. (B) Samples were equilibrated for 3 weeks at 20 °C. (C) Samples were equilibrated at 45 °C for 6 days, and then the signals were monitored at 20 °C.
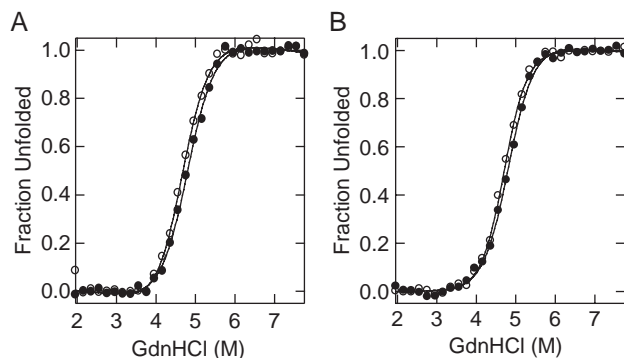
Fig. 3. GdnHCl-induced refolding titration curves obtained by monitoring CD signals at 222 nm (open circles) and the red shift of the maximum emission wavelength excited at 280 nm (open circles) at 20 °C. (A) Samples were equilibrated for 2 days at 20 °C. (B) Samples were equilibrated for 1 week at 20 °C.

via the accumulation of stable intermediates with a significant secondary structure but without tertiary contacts. To achieve complete equilibrium, the samples were incubated at 45 °C for 6 days (Fig. 2C). The unfolding titration curves measured by fluorescence and CD were superimposed, and both curves were fitted well to the two-state mechanisms (Eq. (1)). These results suggest that no equilibrium intermediates accumulate completely in the equilibrium condition.

Fig. 3 shows the refolding transition curves by diluting the completely unfolded *Tk*-MGMT in 7.2 M GdnHCl to the desired GdnHCl concentrations. In the case of incubation at 20 °C for 2 days, the titration curves measured by CD and fluorescence were identical, and fitted well to the two-state mechanism (Fig. 3A). After further incubation at 45 °C for 6 days, no change was observed in the refolding transition curves (Fig. 3B). These results suggest that refolding equilibrium is much faster than unfolding equilibrium, and that no intermediates accumulate in the refolding pathway.

3.2. Kinetic unfolding

Fig. 4 shows the unfolding progress curves induced by 7.2 M GdnHCl at 50 °C. The data measured by CD at 222 nm were fitted to a double-exponential function (Eq. (3)) (Fig. 4A, B). The data measured by fluorescence were also fitted to a double-exponential function (Fig. 4C, D). The apparent unfolding rates and fraction amplitudes monitored by CD were $2.36 \pm 0.04 \times 10^{-3}$ s^{-1} and $68.9 \pm 1.3\%$ for the slower phase, and $1.17 \pm 0.07 \times 10^{-2}$ s^{-1} and $31.1 \pm 1.3\%$ for the faster phase, respectively. The apparent unfolding rates and amplitudes monitored by fluorescence were $5.74 \pm 0.12 \times 10^{-3}$ s^{-1} and $67.8 \pm 3.2\%$ for the slower phase and $1.46 \pm 0.10 \times 10^{-2}$ s^{-1} and $32.2 \pm 3.1\%$ for the faster phase, respectively. The unfolding monitored by fluores-
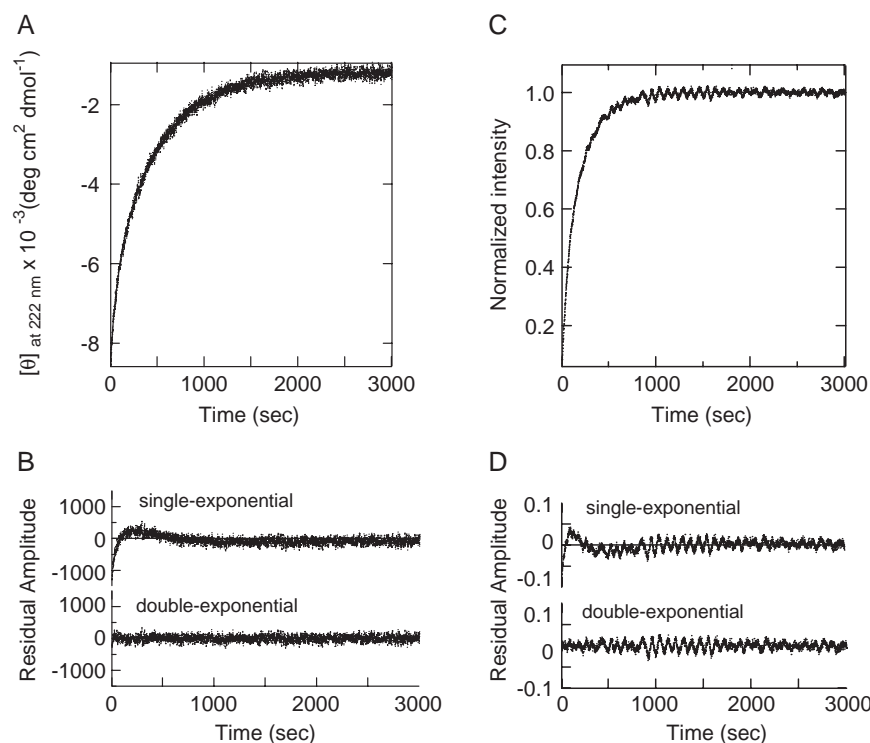

Fig. 4. Representative data of GdnHCl-induced unfolding kinetics of *Tk*-MGMT. The data were recorded by following changes in CD at 222 nm or fluorescence intensity at 355 nm as a result of mixing the folded protein with the final concentrations of 7.2 M GdnHCl. (A) Unfolding kinetics monitored by CD at 222 nm at 50 °C. The solid line was obtained as a least-square fit to a double exponential equation. (B) The residuals for the single or double exponential fit at 50 °C. (C) Unfolding kinetics monitored by fluorescence intensity at 355 nm at 50 °C. The solid line was obtained as a least-square fit to a double exponential fit. (D) The residuals for the single or double exponential fit at 50 °C.
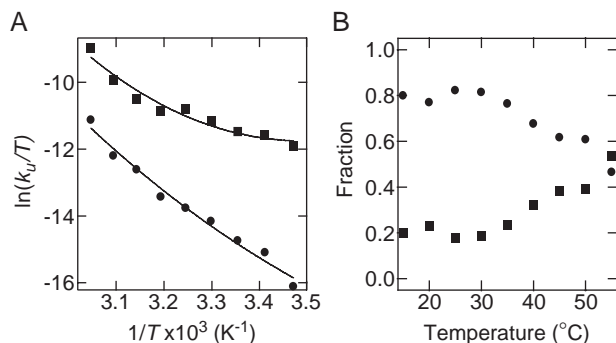
Fig. 5. (A) The temperature dependence of unfolding rate constants in 7.84 M GdnHCl, plotted as an Eyring diagram. The squares and circles represent the data of the faster and the slower phase, respectively. The solid lines were obtained as least-square fits to Eqs. (4) and (5). (B) The temperature dependence of the fractions of the faster phase and the slower phase in 7.84 M GdnHCl.

cence was faster than that monitored by CD, which is consistent with the results of studies on equilibrium. The fraction amplitudes of the faster and slower phases monitored by both probes were almost identical. These results suggest that the unfolding of *Tk*-MGMT is significantly complex, and that each step monitored by CD is the same event as each step monitored by fluorescence.

3.3. Temperature dependence of unfolding kinetics

The apparent rates of GdnHCl-induced unfolding of *Tk*-MGMT were measured by monitoring the CD at 222 nm in 7.84 M GdnHCl at 10 different temperatures from 15 to 55 °C. All data were analyzed by a double exponential function, and the unfolding rate constants and amplitudes were calculated. Fig. 5 shows the Eyring plot for these data.

Non-linearity in the Eyring plots is observed when there is a difference in the heat capacity between the initial state and the transition state [16,17]. In this case, activation parameters, such as $\Delta H^{\ddagger}$, $\Delta S^{\ddagger}$, and $\Delta G^{\ddagger}$, depend on temperature. According to Eqs. (4) and (5), the fast and slow phase had a little curvature (Fig. 5A), resulting in the positive $\Delta C_{p}^{\ddagger}$ of 2.32 ± 0.81 and 1.11 ± 0.85 kJ mol^{-1} K^{-1}. This positive $\Delta C_{p}^{\ddagger}$ implies that, in approaching the transition state of unfolding, an additional surface becomes exposed to the solvent.

$\Delta G_{25\ °C}^{\ddagger}$, $\Delta H_{25\ °C}^{\ddagger}$, and $\Delta S_{25\ °C}^{\ddagger}$ of the fast phase were 87.4 kJ mol^{-1}, 27.6 kJ mol^{-1}, and -201 J mol^{-1} K^{-1}, respectively. These results suggest that the barrier to unfolding is mainly entropic, rather than enthalpic. On the other hand, $\Delta G_{25\ °C}^{\ddagger}$, $\Delta H_{25\ °C}^{\ddagger}$, and $\Delta S_{25\ °C}^{\ddagger}$ of the slow phase were 95.7 kJ mol^{-1}, 77.6 kJ mol^{-1}, and -60.7 J mol^{-1} K^{-1}, respectively. These results suggest that the barrier to unfolding in this step is mainly enthalpic.

3.4. Initial condition test

The observation of at least two kinetic phases during unfolding can be explained either using a sequential model

with an intermediate or using a parallel model [18]. The initial condition test is based on the fact that the unfolding rates for the reactions depend only on the final conditions, while the amplitudes depend on both the final and initial conditions [18–20]. To test whether unfolding reactions are sequential or parallel, the samples were equilibrated at 1.2, 2.4, 3.6, 3.9, 4.2, 4.5, and 4.8 M of the GdnHCl concentrations at 50 °C. Then, the unfolding reaction was initiated by rapidly transferring each sample to a final concentration of 7.2 M GdnHCl at 50 °C, and the unfolding processes were monitored by CD at 222 nm. The obtained unfolding reaction traces were fitted to the double-exponential function, and the amplitudes obtained from the fits were plotted as a function of the starting GdnHCl concentrations (Fig. 6). If the unfolding reaction occurs in a sequential pathway, the amplitude for the faster phase decreases first, and then the amplitude for the slower phase decreases. On the other hand, if the unfolding reaction occurs in a parallel pathway, a simultaneous decrease in both of the amplitudes was observed with midpoints near the GdnHCl concentration corresponding to the equilibrium unfolding transition. These obtained results have been described by the latter model, suggesting that the two unfolding processes of *Tk*-MGMT occur in parallel (Fig. 6).

3.5. Cysteine-labeling reactions

The free thiol group of cysteine reacts with DNTB at an alkaline pH, resulting in the release of one TNB^{-}. The rate of reaction can therefore be monitored by measuring the increase in absorbance at 412 nm due to the release of TNB^{-}. The observed rate of labeling of a cysteine gives the structural information around the cysteine. *Tk*-MGMT has one cysteine residue at the active site. If *Tk*-MGMT has a unique native conformation, the observed labeling process should be followed to a single-exponential function. To confirm the existence of the two native conformations, we monitored the reaction of *Tk*-MGMT with DTNB at 20 °C.
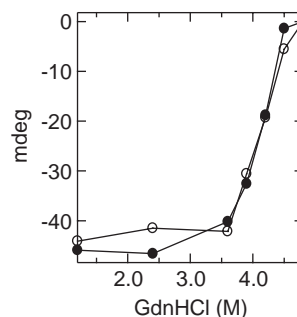

Fig. 6. Initial condition test. Unfolding was initiated by the GdnHCl concentration jump from various concentrations to 7.2 M GdnHCl. The open and closed circles represent the amplitudes of the faster and the slower phase, respectively.

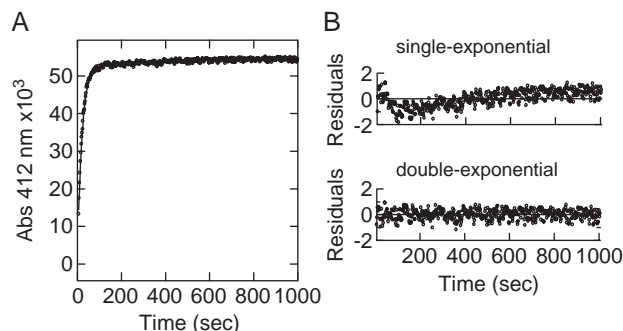   *S. Nishikori et al. / Biophysical Chemistry 116 (2005) 97–104*

Fig. 7. Reaction of DTNB with the reactive center of Cys 141 in *Tk*-MGMT. (A) The reaction was monitored by absorbance at 412 nm in 20 mM Na-phosphate buffer (pH 8.0). (B) The residuals for the single exponential fit (top) and the double-exponential fit (bottom).

Fig. 7 shows the labeling reaction of native *Tk*-MGMT with DTNB monitored by absorbance at 412 nm. The reaction of *Tk*-MGMT with DTNB was biphasic, suggesting that *Tk*-MGMT has two different conformations while retaining active cysteine on the reactive site.

4. Discussion

Importantly, distinct kinetic events during unfolding were identified in this study. The unfolding profiles monitored by CD and fluorescence were biphasic, and 4 distinct unfolding rate constants were obtained. These results suggest that the unfolding reaction consists of at least 4 kinetic steps. Unfolding observed by CD was slower than that observed by fluorescence. In addition, the equilibrium transition curves during unfolding measured by the two spectroscopic probes were not superimposed at low temperatures. These data clearly indicate that the unfolding of *Tk*-MGMT proceeds via at least 4 processes, and that intermediates with a predominantly α-helical structure without tertiary packing accumulate during unfolding. Unfolding intermediates have been found only rarely in earlier studies.

It is particular interesting to note that small globular proteins usually unfold via a single kinetic step in strongly denaturing conditions. It is plausible that no kinetic intermediates accumulate during unfolding because of their low stability under strongly denaturing conditions [21]. As a result, single exponential unfolding kinetic traces without lag phase are normally observed [22–24]. Furthermore, probes of both secondary and tertiary structures usually give rise to very similar rate constants [25], providing evidence for the cooperative process. Recently, the technique of native-state amidehydrogen exchange (HX) has allowed small populations of partially unfolded molecules to characterize under subdenaturing conditions. These equilibrium HX studies show that partially unfolded forms or unfolding intermediates are populated transiently for several proteins including cytochrome *c* [26], RNaseH [21,27], and barster [28]. These structural characterizations of unfolding

intermediates give information about the transition state of unfolding. It is worth mentioning that the unfolding of *Tk*-MGMT was non-cooperative, and that intermediates apparently accumulate during unfolding even in strongly denaturing conditions using CD and fluorescence.

Observation of multiple unfolding steps could result either from a sequential unfolding process or a parallel unfolding process. The initial condition test is a good method of distinguishing between sequential and parallel pathways [18]. Using this analysis, the two unfolding steps observed by CD measurement are shown to be parallel. Furthermore, to investigate whether or not the parallel pathways result from the heterogeneity of native conformations, cysteine reactivity was analyzed using DTNB. *Tk*-MGMT has only one cysteine residue in the reactive center. As a result, the cysteine reactivity was biphasic, strongly indicating the existence of two native conformations in the physiological condition.

The model for the unfolding of *Tk*-MGMT in 7.2 M GdnHCl at pH 8.0 and 50 °C must explain the following experimental observation. (i) Under the native condition, *Tk*-MGMT comprises at least two populations of molecules. (ii) The two conformations are equilibrated very slowly with each other, and these two conformations unfold through different unfolding pathways. (iii) The loss of tertiary structure and secondary structure occur in 2 steps, and each amplitude of the faster and slower phases obtained by CD is similar to that obtained by fluorescence. (iv) The loss of
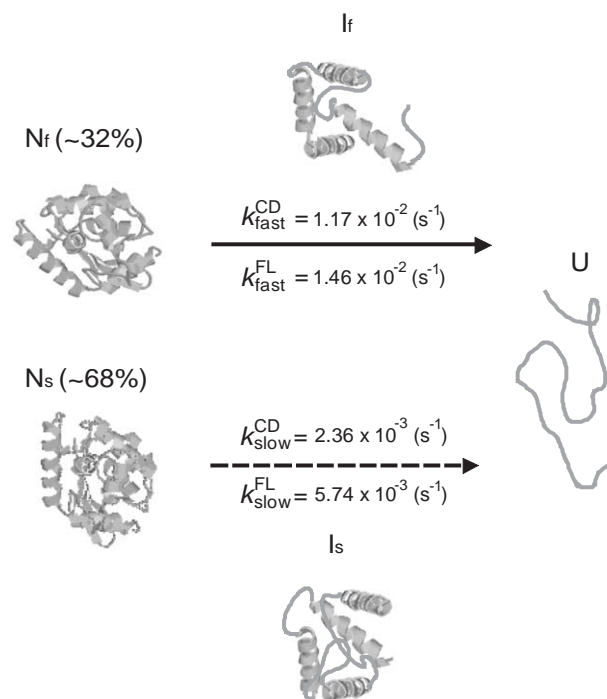

Fig. 8. Unfolding model of *Tk*-MGMT in 7.2 M GdnHCl at 50 °C. k_{fast}^{CD} and k_{slow}^{CD} represent the unfolding rates obtained by monitoring the CD signals of the faster and the slower phase, respectively. k_{fast}^{FL} and k_{slow}^{FL} represent the unfolding rates obtained by monitoring the fluorescence signals of the faster and the slower phase, respectively.

tertiary structure is followed by the loss of secondary structure. (v) Intermediates with an α-helical structure but not tertiary contacts accumulate during unfolding. The deduced unfolding mechanism of Tk-MGMT is shown in Fig. 8. In this mechanism, there are two native conformations under the native condition (N_s and N_f). N_s is the ensemble that unfolds on the slow unfolding pathway, and N_f on the fast unfolding pathway. I_s and I_f are transient intermediates that lose tertiary packing with significant α-helical conformation. Evidence for the accumulation of these molten-globule-like intermediates is provided by equilibrium studies.

Heterogeneity in the native state has been observed for staphylococcal nuclease [29]. It has since then been described for several proteins and is frequently caused by different isomers of prolyl-peptide bonds [30–32]. Tk-MGMT has 7 proline residues, and there are 4 prolines in the loop region. The heterogeneity of the native conformer of Tk-MGMT may be caused by the isomerization of these prolines. Only a single peak could be detected by ion exchange and size exclusion chromatography (data not shown). Therefore, the global structure of these two conformations seems similar. Local structural differences may change the unfolding pathway of Tk-MGMT.

Hyperthermophilic proteins often display different properties from intact proteins when they are expressed in Escherichia coli as recombinant proteins [33–37]. In these studies, hyperthermophilic proteins often form low-activity conformations in the case of expression as recombinant proteins. These low-activity conformations change into high-activity conformations when heated. Although heat-induced structural change has been previously reported for several hyperthermophilic proteins, the details of the mechanism remain unclear. According to our data, we hypothesize that the heat maturation of hyperthermophilic proteins may result from the heterogeneity of the native conformation due to the rugged energy landscape of folding–unfolding.

The temperature dependences of unfolding allow us to interpret the structure of the intermediates and the unfolding mechanism. Activation enthalpy corresponds to the slope of the Eyring plots. Activation entropy was proportional to the intercept with the ordinate (Fig. 5). Even if $\Delta C_p^{\ddagger}$ varies from 0 to 800 J mol^{-1} K^{-1}, it is obvious from Fig. 5 that the difference between the activation free energies of unfolding between the faster phase and the slower phase is largely due to a difference in activation entropy changes. The activation free energy change of the faster phase was entropic, while that of slower phase was enthalpic at low temperatures (Table 1). These results suggest that the transition state species on the two pathways for unfolding have different fundamental structures because the two native conformations seem to be similar to each other. These data are evidence supporting the new view, in which a protein folds or unfolds in random steps so that multiple pathways are available [1–4].

Table 1
Activation parameters of Tk-MGMT at 25 °C for GdnHCl-induced unfolding of Tk-MGMT measured by CD measurement

	$\Delta G^{\ddagger}$ (kJ mol^{-1})	$\Delta H^{\ddagger}$ (kJ mol^{-1})	$\Delta S^{\ddagger}$ (J mol^{-1} K^{-1})	$\Delta C_p^{\ddagger}$ (kJ mol^{-1} K^{-1})
Faster phase	87.4±0.3	27.6±8.8	−201±30	2.32±0.81
Slower phase	95.7±0.3	77.6±9.2	−60±31	1.11±0.85

The slow unfolding of Tk-MGMT allowed us to detect kinetic intermediates and to analyze the complex unfolding mechanism of Tk-MGMT. Due to the significantly long life of intermediates, it is possible to resolve the structures of the unfolding intermediates of Tk-MGMT by NMR, leading to a detailed understanding of the unfolding mechanism of proteins.

Acknowledgement

References

[1] J.N. Onuchic, Z. Luthey-Schulten, P.G. Wolynes, Theory of protein folding: the energy landscape perspective, Annu. Rev. Phys. Chem. 48 (1997) 545–600.

[2] K.A. Dill, H.S. Chan, From levinthal to pathways to funnels, Nat. Struct. Biol. 4 (1997) 10–19.

[3] R.L. Baldwin, The nature of protein folding pathway: the classical versus the new view, J. Biomol. NMR 5 (1995) 103–109.

[4] C.M. Dobson, A. Sali, M. Karplus, Protein folding: a perspective from theory and experiment, Angew. Chem., Int. Ed. 37 (1998) 868–893.

[5] T. Klefhaber, A.M. Labhardt, R.L. Baldwin, Direct NMR evidence for an intermediate preceding the rate-limiting step in the unfolding of ribonuclease A, Nature 375 (1995) 513–515.

[6] C.M. Phillips, Y. Mizutani, R.M. Hochstrasser, Ultrafast thermally induced unfolding of RNase A, Proc. Natl. Acad. Sci. U. S. A. 92 (1995) 7292–7296.

[7] U. Nath, V.R. Agashe, J.B. Udgaonkar, Initial loss of secondary structure in the unfolding of barstar, Nat. Struct. Biol. 3 (1996) 920–923.

[8] F.N. Zaidi, U. Nath, J.B. Udgaonkar, Multiple intermediates and transition states during protein unfolding, Nat. Struct. Biol. 4 (1997) 1016–1023.

[9] S. Ramachandran, B.R. Rami, J.B. Udgaonkar, Measurements of cysteine reactivity during protein unfolding suggests the presence of competing pathways, J. Mol. Biol. 297 (2000) 733–745.

[10] M.M. Leclere, M. Nishioka, T. Yasuda, S. Fujiwara, M. Takagi, T. Imanaka, The O^6-methylguanine-DNA methyltransferase from the hyperthermophilic archaeon Pyrococcus sp. KOD1: a thermostable repair enzyme, Mol. Gen. Genet. 258 (1998) 69–77.

[11] H. Hashimoto, T. Inoue, M. Nishioka, S. Fujiwara, M. Takagi, T. Imanaka, Y. Kai, Hyperthermostable protein structure maintained by intra- and inter-helix ion-pairs in archaeal O^6-methylguanine-DNA methyltransferase, J. Mol. Biol. 292 (1999) 707–716.

[12] K. Shiraki, S. Nishikori, S. Fujiwara, T. Imanaka, M. Takagi, Contribution of protein–surface ion pairs of a hyperthermophilic protein on thermal and thermodynamic stability, J. Biosci. Bioeng. 97 (2004) 75–77.

[13] S. Nishikori, K. Shiraki, K. Yokota, N. Izumikawa, S. Fujiwara, H. Hashimoto, T. Imanaka, M. Takagi, Mutational effects on O^6-methylguanine-DNA methyltransferase from hyperthermophile: contribution of ion-pair network to protein thermostability, J. Biochem. (Tokyo) 135 (2004) 525–532.

[14] S.C. Gill, P.H. von Hippel, Calculation of protein extinction coefficients from amino acid sequence data, Anal. Biochem. 182 (1989) 319–326.

[15] H. Eyring, The activated complex in chemical reaction, J. Chem. Phys. 3 (1935) 107–115.

[16] T. Dams, R. Jaenicke, Stability and folding of dihydrofolate reductase from the hyperthermophilic bacterium *Thermotoga matiritima*, Biochemistry 38 (1999) 9169–9178.

[17] E.R.G. Main, D.F. Fulton, S.E. Jackson, Folding pathway of FKBP12 and characterization of the transition state, J. Mol. Biol. 291 (1999) 429–444.

[18] L.A. Wallance, C.R. Matthews, Sequential vs. parallel protein-folding mechanism: experimental tests for complex folding reactions, Biophys. Chemist. 101–102 (2002) 113–131.

[19] C. Tanford, Protein denaturation. Part A, Adv. Protein Chem. 23 (1968) 121–217.

[20] P.J. Hagerman, R.L. Baldwin, A quantitative treatment of the kinetics of the folding transition of ribonuclease A, Biochemistry 15 (1976) 1462–1473.

[21] J. Juneja, J.B. Udgaonkar, Characterization of the unfolding of ribonuclease A by a pulsed hydrogen exchange study: evidence for competing pathways for unfolding, Biochemistry 41 (2002) 2641–2654.

[22] S. Segawa, M. Sugihara, Characterization of the transition state of lysozyme unfolding: I. Effect of protein–solvent interactions on the transition state, Biopolymers 23 (1984) 2473–2488.

[23] S.E. Jackson, A.R. Fersht, Folding of chymotrypsin inhibitor 2: 1. Evidence for a two-state transition, Biochemistry 30 (1991) 10428–10435.

[24] A. Nicholls, K.A. Sharp, B. Honig, Protein folding and association: insights from the interfacial and thermodynamic properties of hydrocarbons, Proteins 11 (1991) 281–296.

[25] K. Yamasaki, K. Ogasahara, K. Yutani, M. Oobatake, S. Kanaya, Folding pathway of *Escherichia coli* ribonuclease HI: a circular dichroism, fluorescence, and NMR study, Biochemistry 34 (1995) 16552–16562.

[26] Y. Bai, T.R. Sosnick, L. Mayne, S.W. Englander, Protein folding intermediates: native-state hydrogen exchange, Science 269 (1995) 192–197.

[27] A.K. Chamberlain, T.M. Handel, S. Marqusee, Detection of rare partially folded molecules in equilibrium with the native conformation of RNaseH, Nat. Struct. Biol. 9 (1996) 782–787.

[28] A.K. Bhuyan, J.B. Udgaonkar, Two structural subdomains of barstar detected by rapid mixing NMR measurement of amide hydrogen exchange, Proteins 30 (1998) 295–308.

[29] J.L. Markly, M.N. Williams, O. Jardetzky, Nuclear magnetic resonance studies of the structure and binding sites of enzymes: XII. A conformational equilibrium in staphylococcal nuclease involving a histidine residues, Proc. Natl. Acad. Sci. U. S. A. 65 (1970) 645–651.

[30] W.J. Chazin, J. Kordel, T. Drakenberg, E. Thulin, P. Brodin, T. Grundstrom, S. Forsen, Proline isomerism leads to multiple folded conformations of calbindinD9k: direct evidence from two-dimensional 1H NMR spectroscopy, Proc. Natl. Acad. Sci. U. S. A. 86 (1989) 2195–2198.

[31] Y. Feng, W.F. Hood, R.W. Forgey, A.L. Abegg, M.H. Caparon, B.R. Thiele, Multiple conformations of a human interleukin-3 variant, Protein Sci. 6 (1997) 1777–1782.

[32] F. Rousseau, J.W. Schymkowitz, M. Sanchez del Pino, L.S. Itzhaki, Stability and folding of the cell cycle regulatory protein, p13(suc1), J. Mol. Biol. 284 (1998) 503–519.

[33] C. Kobayashi, Y. Suga, K. Yamamoto, T. Yomo, K. Ogasahara, K. Yutani, I. Urabe, Thermal conversion from low- to high-activity forms of catalase I from *Bacillus stearothermophilus*, J. Biol. Chem. 272 (1997) 23011–23016.

[34] R.N.Z.A. Rahman, S. Fujiwara, M. Takagi, S. Kanayama, T. Imanaka, Effect of heat treatment on proper oligomeric structure formation of thermostable glutamate dehydrogenase from a hyperthermophilic archaeon, Biochem. Biophys. Res. Commun. 241 (1997) 646–652.

[35] M.A. Siddiqui, S. Fujiwara, M. Takagi, T. Imanaka, In vitro heat effect on heterooligomeric subunit assembly of thermostable indolepyruvate ferredoxin oxidoreductase, FEBS Lett. 434 (1998) 372–376.

[36] T. Yamamoto, K. Shiraki, S. Fujiwara, M. Takagi, K. Fukui, T. Imanaka, In vitro heat effect on functional and conformational changes of cyclodextrin glucanotransferase from hyperthermophilic archaea, Biochem. Biophys. Res. Commun. 265 (1999) 57–61.

[37] N. Izumikawa, K. Shiraki, S. Nishikori, S. Fujiwara, T. Imanaka, M. Takagi, Biophysical analysis of heat-induced structural maturation of glutamate dehydrogenase from a hyperthermophilic archaeon, J. Biosci. Bioeng. 97 (2004) 305–309.